PRAMANA
— journal of
physics

Vol. 75, No. 6
December 2010
pp. 1221–1232

Femtosecond laser-fabricated microstructures in bulk poly(methylmethacrylate) and poly(dimethylsiloxane) at 800 nm towards lab-on-a-chip applications

K L N DEEPAK[1], S VENUGOPAL RAO[2] and D NARAYANA RAO[1,*]
[1]School of Physics, [2]Advanced Centre of Research in High Energy Materials (ACRHEM), University of Hyderabad, Hyderabad 500 046, India
[*]Corresponding author. E-mail: dnrsp@uohyd.ernet.in

Abstract. Laser direct writing technique is employed to fabricate microstructures, including gratings (buried and surface) and two-dimensional photonic crystal-like structures, in bulk poly(methylmethacrylate) (PMMA) and poly(dimethylsiloxane) (PDMS) using ∼100 femtosecond (fs) pulses. The variation of structure size with different writing conditions (focussing, speed and energy) was investigated in detail. Diffraction efficiencies of the gratings were calculated and the changes in diffraction efficiency (DE) as a function of period, energy and scanning speed were evaluated. Highest diffraction efficiencies of 34% and 10%, for the first order, were obtained in PMMA and PDMS respectively. Heat treatment of these gratings demonstrated small improvement in the diffraction efficiency. Several applications resulting from these structures are discussed. Fs modification in PMMA and PDMS demonstrated emission when excited at a wavelength of 514 nm. We attempted to prepare buried waveguides in PMMA with higher refractive index at the core. We have successfully fabricated branched and curved structures in PMMA and PDMS finding impending applications in microfluidics.

Keywords. Laser direct writing; diffraction gratings; refractive index change; emission.

PACS Nos 87.85.Va; 82.50.Pt; 42.82.Gw

1. Introduction

Ultrashort pulses provided by femtosecond lasers when focussed tightly in a dielectric or polymer material creates highly localized refractive index changes by invoking the nonlinearities due to large peak intensities resulting in multiphoton absorption within the focal volume. Therefore, fs direct writing facilitates large penetration depths and genuine 3D structuring [1–3]. A polymer material such as PMMA, which is the base material for polymer optical fibres and other devices, makes its possible to manufacture inexpensive and rugged components and devices. Femtosecond lasers are now being widely used in the internal modification

of transparent materials. Because of multiphoton absorption process, the interaction between the fs laser and the material occurs only in the vicinity of focal spot, leaving the surface of the material intact. One of the most important applications of this ability to modify the refractive index (RI) is in the field of photonics [4–7]. A variety of three-dimensional structures such as waveguides, couplers and gratings have been fabricated in PMMA and PDMS, which are useful for photonic and microfluidic applications [8–22]. A comprehensive understanding of the interaction of femtosecond pulses with these materials with particular attention to their pulse duration, energies, shapes, focussing conditions etc. is indispensable for arriving at optimum writing conditions to achieve device-quality microstructures. Herein we present our results on the studies of various structures, effect of different writing conditions using ∼100 fs pulses and their physical and optical characterization.

2. Experimental details

2.1 *Materials preparation*

In our experiments we have written microstructures in PMMA purchased locally, PMMA purchased from Goodfellow, USA and home-made PDMS films. PMMA and PDMS samples with thicknesses of 1 mm and 6 mm, respectively, were used in all our experiments. These samples were cut into 1 cm × 1 cm dimensions using polymer cutter. Edges were polished using alumina powder and polishing sheets of different grades. Before irradiating with fs pulses, these samples were sonicated for 1 h in distilled water to remove dust and unwanted polishing powder. To characterize the microstructures after fabrication using laser confocal microscope and/or scanning electron microscope (SEM), these samples were once more polished till cross-sections were visible in the microscope and later sonicated. For SEM studies we coated the samples with gold using sputtering technique.

2.2 *Material properties and measurements*

These polymers are transparent to visible light and do not have any absorption peak in the visible region. The tensile strength of PDMS is ∼2.24 MPa while for PMMA it is ∼70 MPa implying that it is easier to physically modify PDMS (compared to PMMA) using fs pulses. For measuring widths and depths of the microstructures, we used confocal microscope and SEM. Emission measurements were also carried out using the same confocal microscope. For measuring the percentage of DE, we used a He–Ne laser and measured the power diffracted into various orders using a handheld power meter. First-order diffraction efficiency is defined as the ratio of power diffracted into first order to the incident power.

3. Results and discussion

Microstructures are fabricated using a Ti:sapphire oscillator-amplifier system operating at a wavelength of 800 nm delivering ∼100 fs pulses, ∼1 mJ energy with a repetition rate of 1 kHz. The transform-limited nature of the pulses is confirmed from the time-bandwidth product. Three translational stages (Newport) are used

to translate the sample in X, Y and Z directions. Laser energy is varied using the combination of half-wave plate and a polarizer. The writing is performed in the transverse geometry with polarization of the input beam perpendicular to the translation of the sample. We have used 40× and 20× microscopic objectives (Olympus, Numerical Aperture (NA) of 0.65 and 0.4, respectively) in our focussing experiments. Spot sizes are calculated using the formula $D = 1.22\lambda/\mathrm{NA}$, where D is the diameter of the focussed spot, $\lambda = 800$ nm and NA is the numerical aperture of the microscopic objective. The theoretical spot sizes are found to be ∼1.5 and ∼2.4 μm, respectively, for 40× and 20× objectives. The values of energies mentioned hereafter are measured before all the optical components in the experiment, implying the actual values at the focus could be lesser by at least 20–30%.

The energy of an 800 nm photon corresponds to 1.55 eV while the optical band gap of pure PMMA is ∼4.58 eV. This implies that the nonlinear process involves at least three photons being responsible for structural modification at the focal volume [10]. Three possible mechanisms [1,21] such as tunnelling, intermediate and multiphoton ionizations are likely to take place when transparent material interacts with femtosecond pulses. The Keldysh parameter which provides information about the dominant mechanism, is defined as $\gamma = (\omega/e)(m \times c \times n \times \varepsilon_0 \times E_\mathrm{g}/I)$ where ω is the laser frequency, I is the laser peak intensity at the focus, m and e are the reduced mass and charge of the electron, respectively, and c is the velocity of light, n is the refractive index of the material, E_g is the band gap of the material and ε_0 is the permittivity of free space. For our studies (PMMA) we realized that tunnelling as the mechanism responsible for fs-laser induced changes as the Keldysh parameter is <0.5 for structures written using 40×. Similar calculations were carried out for 20× objective and it is found that tunnelling mechanism plays a major role.

Initially we fabricated microstructures in PMMA using single and double scan methods using both 40× and 20× objectives. For reproducibility we obtained two sets of structures in PMMA and the data are in good agreement in both the cases. Typical confocal images and variation of the width with input energy for these structures are shown in figures 1a and 1b, respectively. Similar structures were achieved in PDMS (using 40× and 20× objective lenses) and figures 1c and 1d show the structures and plots of structure width vs. input energy, respectively. As expected, the structure width is found to be increasing with input energy and the number of scans. Since the 20× objective spot size is more than 40× objective, structures written at the same energy with the 40× and 20× are compared and the width is found to be more in PDMS than in PMMA, as PDMS is a relatively soft material compared to PMMA. Before fabricating the two-dimensional gratings we fabricated several microstructures on the surface of PMMA. To understand whether the modification is a void-type or hybrid-type (defined as void regions mixed with regions of pure refractive index change) or regions with only refractive index change, we collected the SEM data of these structures. Figures 2a and 2b show the SEM images of the fabricated microstructures. Through confocal microscope we could not clearly establish the kind of modification occurred at the focal volume. But, it is clear when we viewed them through SEM. Figures 2a and 2b clearly show grooves in the irradiated region indicating that the fabricated structure is of void-type. The microstructures are a result of the melting and re-solidification of polymer at high temperatures created by these intense, short pulses. We observed splitting of the

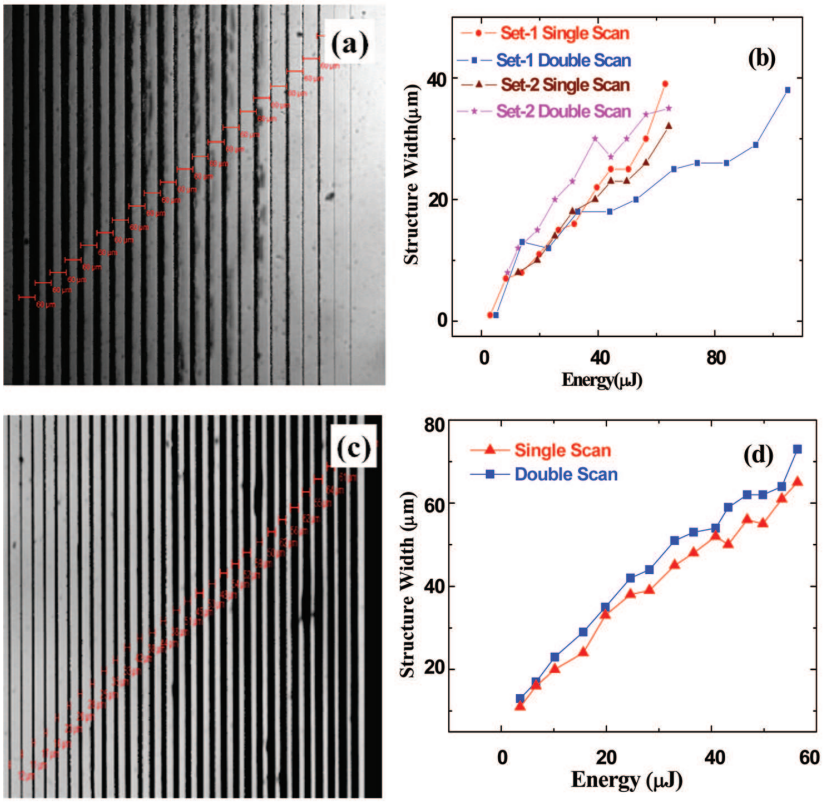

Figure 1. (**a**) Microstructures obtained in PMMA using 40× objective in SET-1 confocal microscope image of the structures fabricated (right to left structures were written with increasing energy in single- and double-scan methods – Spacing between structures = 60 μm). (**b**) Plot of structure width vs. energy in SET-1 and SET-2 experiments. (**c**) (Right to left structures were written with decreasing energy in single- and double-scan methods) Microstructures written in PDMS using 40× objective (spacing between structures = 100 μm). (**d**) Plot of structure width vs. energy in PDMS written with 40× objective. Scanning speed is 1 mm/s for all the structures shown here.

microstructures written with 80–50 μJ (decreasing) energies as illustrated in the SEM pictures (figure 2b). The splitting behaviour could be due to the damage in the 40× objective which we realized later after careful observation of the transmitted He–Ne laser beam in the far-field. At lower energies (<570 nJ) we have not observed any grooves. We expect smooth refractive index change near the edges of all the structures as the energy at the ends of Gaussian beam is sufficiently low (<1 μJ).

We fabricated diffraction gratings at energies >50 μJ in PMMA (local) and compared their diffraction efficiency (DE) with scanning speed, average energy and grating period. Table 1 enlists the different conditions of fabrication and their diffraction efficiencies. We follow the following abbreviations for different structures.

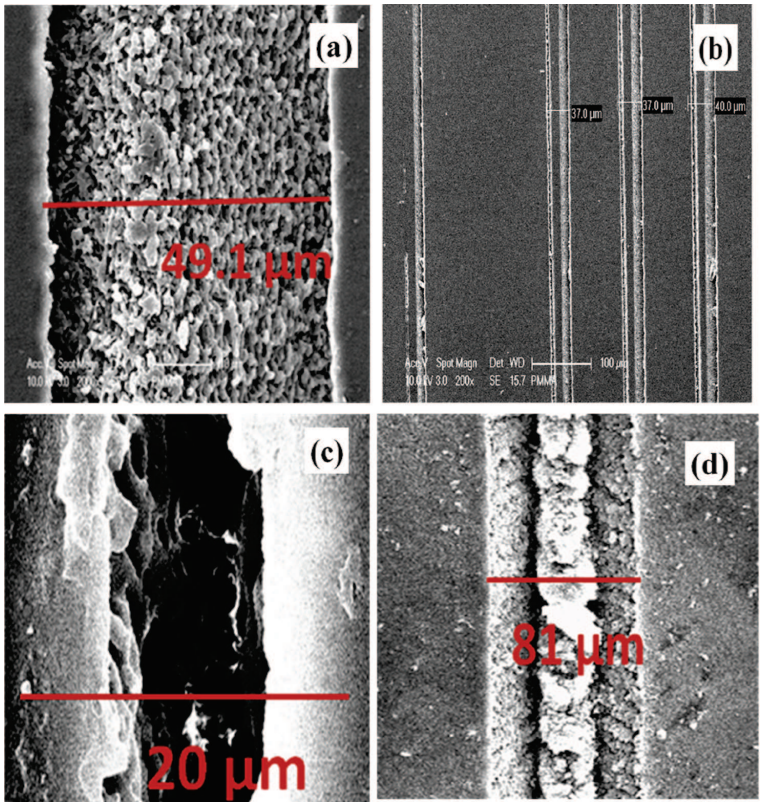

Figure 2. (**a**) Surface microstructures fabricated in PMMA at 150 μJ energy (width = 49.1 μm). (**b**) 80–50 μJ energies from right to left in steps of 10 μJ energy (scale bar = 100 μm). (**c**) SEM image of the surface structure written at 54 μJ in PMMA (width = 20 μm). (**d**) SEM images of PDMS surface where structure is written at 54 μJ (width = 81 μm). 40× objective is used with 1 mm/s speed for all the structures shown.

First four letters represent the material (PMMA or PDMS). Next two letters represent grating type: whether buried grating (BG) or surface grating (SG). Next two numbers represent a particular writing condition (period, energy and scanning speed). Last character represents whether it is written at higher energy (H) or lower energy (L). All these gratings were fabricated at high energies and hence the modification was purely void-type which was confirmed by SEM images of cross-sections of such structures. We obtained maximum DE for grating PMMABG11H written with 50 μJ, 250 μm/s, and 15 μm period (DE of $\sim$34%). We fabricated diffraction gratings (hybrid-type) at low energies that consisted of a void region surrounded by a region of refractive index (RI) change. Figures 2c–d clearly show SEM images of PMMA (Goodfellow) and PDMS surface structures. Intermediate energies at the focal spot, possessing high peak intensities, eject the debris and this phenomenon is demonstrated through the SEM images of the surface structures.

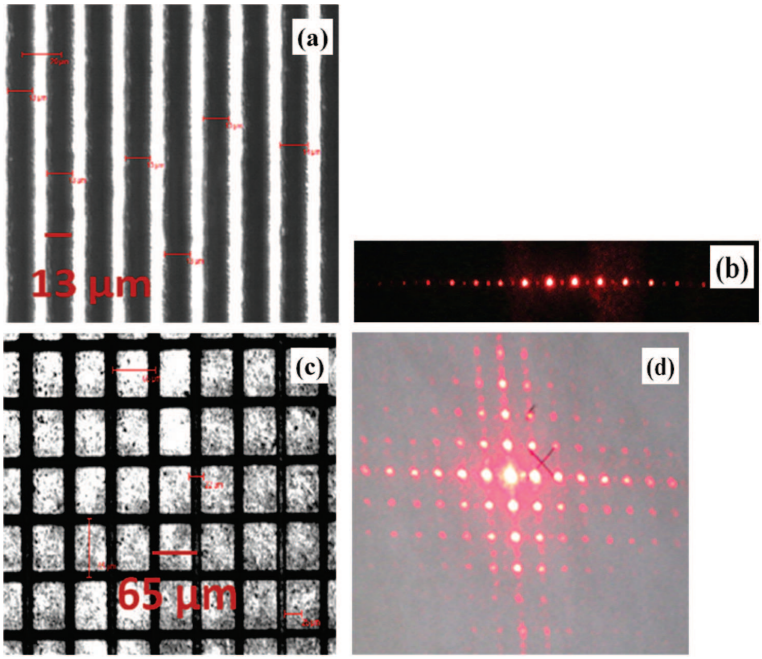

Figure 3. (**a**) Confocal image of a buried grating in PDMSBG02L (3 μJ, 500 μm/s, 20 μm period, 13 μm width). (**b**) Diffraction pattern for the grating depicted in (a). (**c**) Confocal image of PDMS (energy = 30 μJ, period = 65 μm, width = 30 μm, scanning speed = 1 mm/s). (**d**) Diffraction pattern of grating depicted in (c). 40× objective is used for all the structures depicted.

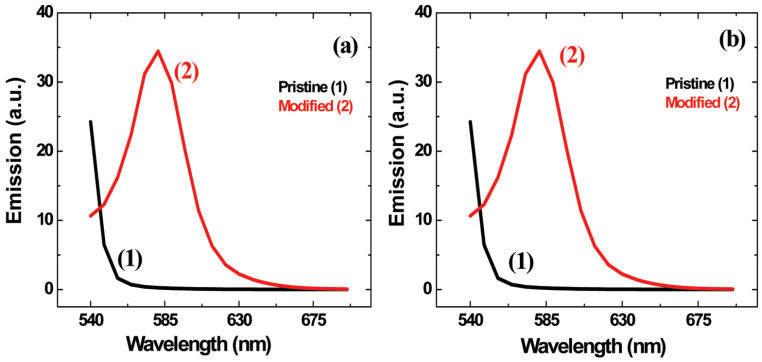

Figure 4. (**a**) Plot of emission with wavelength in PMMA. (**b**) Plot of emission with wavelength in PDMS. Excitation wavelength = 514 nm, energy = 15 μJ, speed = 0.05 mm/s.

For buried structures, and at intermediate energies, there is a possibility of debris settling within the structure as it cannot escape. These are hybrid gratings with void regions followed by high-density region and pristine region and therefore can

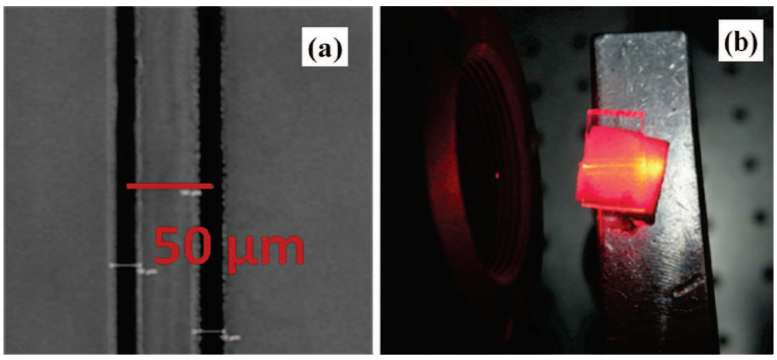

Figure 5. (**a**) Confocal microscope image of SS3 with separation 50 μm (scale bar) and (**b**) coupling of 633 nm light.

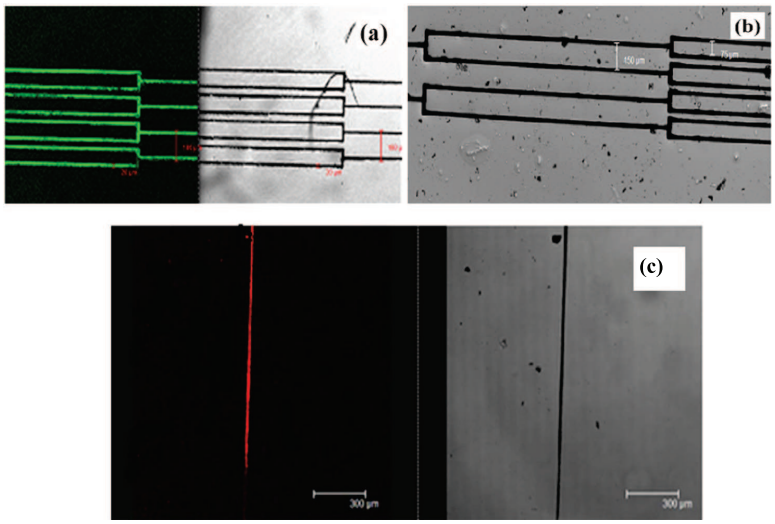

Figure 6. (**a**) 1 : 8 structure fabricated in PMMA. Pseudogreen colour shows the emission from the modified region at an excitation of 488 nm (size of the structure = 15 μm). (**b**) 1 : 8 branched structures in PDMS (size of the structure = 25 μm). (**c**) Fluorescence of rhodamine B solution injected into the structure and excited at 543 nm in PMMA. 40× objective is used with writing parameters of 15 μJ, 0.05 mm/s speed for all the structures shown.

be considered as double grating structures leading to a weak diffraction pattern being observed along with the strong diffraction pattern.

We also attempted fabricating similar buried gratings in PDMS at different writing conditions. To the best of our knowledge, we report maximum diffraction efficiency (∼10%) in PDMSBG01L (3 μJ, 1 mm/s, 15 μm period). Cho *et al* [20] have reported a maximum diffraction efficiency of 6% in similar structures. They used 130 fs pulses, 1 kHz repetition rate with an NA of 0.85. Figures 3a and b show the

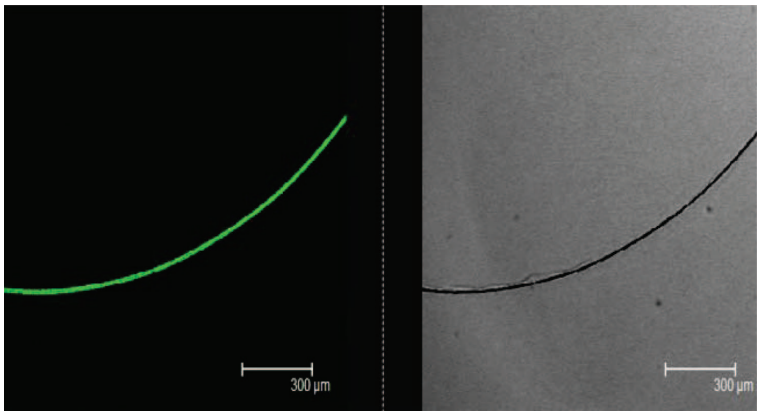

Figure 7. Part of the shape '8' fabricated in PMMA. Pseudogreen colour shows emission from the modified region excited at 488 nm. As image is large, only parts of image are captured (scale bar = 300 μm).

Table 1. Grating data written with high energies for PMMA (local grade) using 40× objective.

Terminology	Average energy (μJ)	Speed (μm/s)	Period (μm)	First order % DE
PMMABG01H	150	500	8	14.3
PMMABG02H	200	500	8	3.5
PMMABG03H	200	500	10	No pattern
PMMABG04H	200	800	10	No pattern
PMMABG05H	200	1000	10	No pattern
PMMABG06H	60	500	50	14.0
PMMABG07H	60	500	25	20.0
PMMABG08H	60	500	10	5.6
PMMABG09H	60	500	5	No pattern
PMMABG10H	50	1000	15	8.9
PMMABG11H	50	250	15	34.0
PMMABG12H	50	750	15	No pattern
PMMABG13H	50	500	15	6.5

confocal image of PDMSBG02L, and its diffraction pattern. The refractive index change in the modified region was calculated using the formula [12,21].

$$\Delta n = \lambda \cos \Theta \tanh^{-1}(\sqrt{\eta})/\pi d,$$

where Δn is the refractive index change, λ is the wavelength of light used, η is the diffraction efficiency, d is the grating thickness/depth, Θ is the angle between normal and incident direction of light used which is equal to 0°. We fabricated surface gratings and two-dimensional gratings on PMMA and PDMS. Figures 3c and d show the two-dimensional grid and the diffraction pattern.

Table 2. Data of DE of various gratings after heat treatment in PMMA and PDMS.

Sample name	Particulars of heat treatment	% DE for 0th order	% DE for 1st order	% DE for 2nd order
PMMABG01L	Initial	47	7.6	2.8
(40×, 3 μJ,	Heat treatment at	61	6.1	6.1
1 mm/s, 15 μm	70°C for 384 h			
period)	Heat treatment at	59	4.84	1.24
	80°C after 552 h			
PMMABG02L	Initial	68	4.72	2.8
(40×, 3 μJ,	Heat treatment at	80	3.1	3.1
0.5 mm/s, 20 μm	70°C for 384 h			
period)	Heat treatment at	81	1.8	1.2
	80°C after 552 h			
PMMABG03L	Initial	–	–	–
(20×, 6 μJ,	Heat treatment at	0.58	0.39	0.39
1 mm/s, 20 μm	70°C for 384 h			
period)	Heat treatment at	7.61	3.4	0.82
	80°C after 552 h			
PMMASG01L	Initial	1.83	0.83	0.3
(40×, 3 μJ,	Heat treatment at	13.27	2.79	0.67
1 mm/s, 18 μm	70°C for 384 h			
period)	Heat treatment at	88.27	2.37	0.21
	80°C after 552 h			
PMMASG02L	Initial	46.83	5.83	2.17
(40×, 5 μJ,	Heat treatment at	51.73	5.1	2.4
1 mm/s, 25 μm	70°C for 384 h			
period)	Heat treatment at	58.02	6.07	2.4
	80°C after 552 h			
PDMSBG01L	Initial	18	10	1.66
(40×, 3 μJ,	Heat treatment at	21	9.83	9.83
1 mm/s, 15 μm	70°C for 384 h			
period)	Heat treatment at	20	9.3	0.55
	80°C after 552 h			
PDMSBG02L	Initial	9.3	7.7	3.1
(40×, 3 μJ,	Heat treatment at	12	7.24	7.24
0.5 mm/s, 20 μm	70°C for 384 h			
period)	Heat treatment at	11	6.54	2.95
	80°C after 552 h			

Hirono *et al* [22] have reported increment in diffraction efficiency from 1.9 to 72% after heat treatment at 70°C for 500 h. They reported the increment as due to an increase in induced refractive index change through volume contraction in the irradiated area after heating. Our studies, however, indicated only a small increase in the diffraction efficiencies as shown in table 2. Initially we heated buried and surface gratings at 70°C for 384 h and later heated samples at 80°C for 552 h to improve efficiencies. In buried gratings in PMMA, we observed no appreciable

Table 3. Data of the double line structures used for light guiding applications (40× objective used).

Terminology	Energy (μJ)	Scanning speed (μm/s)	Period (μm)	Width of each structure (μm)	Gap between two structures (μm)
SS1	30	1000	20	18	2
SS2	30	1000	30	14	16
SS3	30	1000	50	18	32
SS4	30	1000	10	Merged lines with overall width 30 μm	

change in the percentage of diffraction efficiency contrary to the results of Hirono *et al* because the type of gratings that we created is different and mainly due to voids, whereas in their case the gratings were of pure refractive index type. Similar results were obtained in PDMS. But in surface gratings of PMMA, we observed slight enhancement. In PMMABG03L (achieved with low energy), we have not observed any diffraction pattern immediately after fabrication, which was mainly due to overlap of the microstructures. This was also confirmed by the confocal images. After heat treatment however, we observed diffraction pattern possibly due to contraction of the modified regions, as explained by Hirono *et al*. For this particular grating we observed an efficiency of 0.39% after first heating and the efficiency surged to 3.4% on further heating (second heat tratment). In other cases the efficiency of heat-treated gratings was lower than the original ones probably because of the degradation of the samples and/or gratings which require further investigation.

We observed emission from the fs-modified regions of PMMA and PDMS when excited at a wavelength of 514 nm. Figure 4a shows emission from a single structure of PMMA and figure 4b shows the emission from PDMS structure. The observed emission could be from either or a combination of (a) propagating free radicals generated during the exposure to fs pulses, (b) defects formed during the fs writing process, (c) micro-/nano-structured material obtained after the irradiation (figure 2a). Further investigations are in progress to accurately pinpoint the mechanism responsible for this emission.

To demonstrate the versatility of fs direct writing technique we fabricated four parallel structures whose parameters are tabulated in table 3. The exposed regions are expected to form voids with the energies used for writing. Our aim was to create regions of higher refractive index surrounded by regions of lower refractive index for waveguiding applications. If two such structures are fabricated close enough (few microns separation for single-mode waveguiding) light can be guided. We used a He–Ne laser for coupling the light into such a structure. Figure 5a shows the confocal image of a typical structure and light propagation captured by a CCD camera. Out of four structures fabricated, three were found to be guiding light except the last one which is due to the merging of structures. As these structures are buried, portions above and below the central waveguiding region possess same refractive index as that of the substrate making it more like a 2D waveguide. To create a complete 3D waveguide, top and bottom regions also need to be structurally

modified, which we plan to implement in future. As there is no confinement in all the directions we expect higher propagation losses in our case compared to smooth refractive index structures fabricated inside the surface. Efforts are in progress to quantify these losses.

We have also fabricated 1 : 8 branched structures on the surface useful for microfluidic applications. Figures 6a and b show such branched structures in PMMA and PDMS, respectively. We demonstrated capillary action in the structures of PMMA and PDMS by injecting the rhodamine B solution into the structures. We excited the channels with 543 nm radiation and observed fluorescence which is depicted in figure 6c. We have also demonstrated the possibility of fabricating complex structures such as '8' which has curved shape using the present technique. As the fabricated structure was large, only a part of the curve is shown in figure 7.

4. Conclusions

In conclusion we have achieved several buried and surface microstructures in PMMA and PDMS using fs laser pulses. We established the dependence of diffraction efficiency on average energy, scanning speed and period. We achieved highest diffraction efficiencies of the gratings obtained in PMMA and PDMS compared to earlier studies with similar writing conditions. We were successful in enhancing the diffraction efficiency of few gratings marginally through heat treatment below the glass transition temperature. Emission in the fs-modified regions in PMMA and PDMS was demonstrated when excited at a wavelength of 514 nm. We attempted 2D structures towards waveguide applications in PMMA. We also fabricated branched structures in PMMA and PDMS which have practical applications in microfluidics. We have demonstrated the possibility of fabricating complex structures.

Acknowledgements

Financial support from Department of Science and Technology (DST), India through a project, SR/S2/LOP-11/2005, is gratefully acknowledged. D Narayana Rao and S Venugopal Rao acknowledge Council for Scientific and Industrial Research (CSIR) for funding. K L N Deepak acknowledges CSIR for SRF.

References

[1] C B Schaffer, A Brodeur and E Mazur, *Meas. Sci. Tech.* **12**, 1784 (2001)
[2] R R Gattass and E Mazur, *Nat. Phot.* **2**, 219 (2008)
[3] J Kruger and W Kautek, *Adv. Poly. Sci.* **168**, 247 (2004)
[4] D Homoelle, S Wielandy, A L Gaeta, N F Borrelli and C Smith, *Opt. Lett.* **24**, 1311 (1999)
[5] Y Li, W Watanabe, K Yamada, T Shinagawa, K Itoh, J Nishii and Y Jiang, *Appl. Phys. Lett.* **80**, 1508 (2002)
[6] J W Chan, T R Huser, S H Risbud, J S Hayden and D M Krol, *Appl. Phys. Lett.* **82**, 2371 (2003)

[7] K Minoshima, A M Kowalevicz, I Hartl, E P Ippen and J G Fujimoto, *Opt. Lett.* **26**, 1516 (2001)
[8] P J Scully, D Jones and D A Jaroszynski, *J. Opt. A: Pure Appl. Opt.* **5**, S92 (2003)
[9] A Baum, P J Scully, M Basanta, C L P Thomas, P R Fielden, N J Goddard, W Perrie and P R Chalker, *Opt. Lett.* **32**, 190 (2007)
[10] A Baum, P J Scully, W Perrie, D Jones, R Issac and D A Jaroszynski, *Opt. Lett.* **33**, 651 (2008)
[11] A Baum, P J Scully, W Perrie, M Sharp, K G Watkins, D Jones, R Issac and D A Jaroszynski, *Proc. of the 8th International Symposium on Laser Precision Microfabrication*, 2007, pp. 1–5
[12] C Wochnowski, Y Cheng, K Meteva, K Sugioka, K Midorikawa and S Metev, *J. Opt. A: Pure Appl. Opt.* **7**, 493 (2005)
[13] H Mochizuki, W Watanabe, R Ezoe, T Tamaki, Y Ozeki, K Itoh, M Kasuya, K Matsuda and S Hirono, *Appl. Phys. Lett.* **92**, 091120 (2008)
[14] Z Nie, H Lee, H Yoo, Y Lee, Y Kim, K S Lim and M Lee, *Appl. Phys. Lett.* **94**, 111912 (2009)
[15] S Sowa, W Watanabe, T Tamaki, J Nishii and K Itoh, *Opt. Express* **14**, 291 (2006)
[16] D Day and M Gu, *Opt. Express* **13**, 5939 (2005)
[17] A Zoubir, C Lopez, M Richardson and K Richardson, *Opt. Lett.* **29**, 1840 (2004)
[18] S K Sia and G M Whitesides, *Electrophoresis* **24**, 3563 (2003)
[19] A C Siegel, D A Bruzewicz, W B Weibel and G M Whitesides, *Adv. Mater.* **19**, 727 (2007)
[20] S H Cho, W S Chang, K R Kim and J W Hong, *Opt. Commun.* **282**, 1317 (2009)
[21] K L N Deepak, D Narayana Rao and S Venugopal Rao, *Appl. Opt.* **49**, 2475 (2010)
[22] S Hirono, M Kasuya, K Matsuda, Y Ozeki, K Itoh, H Mochizuki and W Watanabe, *Appl. Phys. Lett.* **94**, 241122 (2009)